



Article

Impact of Engine Inertia on P2 Mild HEV Fuel Consumption

Gulnora Yakhshilikova ¹, Sanjarbek Ruzimov ^{1,2,*}, Andrea Tonoli ³ and Akmal Mukhitdinov ⁴

¹ Department of Mechanical and Aerospace Engineering, Turin Polytechnic University in Tashkent, Tashkent 100095, Uzbekistan; gulnora.yakhshilikova@polito.it

² Department of Traffic Engineering, Kimyo International University in Tashkent, Tashkent 100121, Uzbekistan

³ Department of Mechanical and Aerospace Engineering, Politecnico di Torino, 10129 Torino, Italy; andrea.tonoli@polito.it

⁴ Department of Vehicle Engineering, Tashkent State Transport University, Tashkent 100167, Uzbekistan; akmal_a@tstu.uz

* Correspondence: s.rozimov@kiut.uz

Abstract: The energy management system (EMS) of a hybrid electric vehicle (HEV) is an algorithm that determines the power split between the electrical and thermal paths. It defines the operating state of the power sources, i.e., the electric motor (EM) and the internal combustion engine (ICE). It is therefore one of the main factors that can significantly influence the fuel consumption and performance of hybrid vehicles. In the transmission path, the power generated by the ICE is in part employed to accelerate the rotating components of the powertrain, such as the crankshaft, flywheel, gears, and shafts. The main inertial components are the crankshaft and the flywheel. This additional power is significant during high-intensity acceleration. Therefore, the actual engine operation is different from that required by the power split unit. This study focuses on exploring the influence of engine inertia on HEV fuel consumption by developing a controller based on an equivalent consumption minimisation strategy (ECMS) that considers crankshaft and flywheel inertia. The optimal solution obtained by the ECMS controller is refined by incorporating the inertia effect of the main rotating components of the engine into the cost function. This reduces the engine operation during high inertial torque transient phases, resulting in a decrease in vehicle CO₂ emissions by 2.34, 2.22, and 1.13 g/km for the UDDS, US06, and WLTC driving cycles, respectively.

Keywords: hybrid electric vehicle; energy management system; equivalent consumption minimisation; optimal torque split; engine inertia



Citation: Yakhshilikova, G.;

Ruzimov, S.; Tonoli, A.;

Mukhitdinov, A. Impact of Engine Inertia on P2 Mild HEV Fuel

Consumption. *World Electr. Veh. J.*

2024, 15, 220. [https://doi.org/](https://doi.org/10.3390/wevj15050220)

10.3390/wevj15050220

Academic Editors: Davide

Tavernini and Basilio Lenzo

Received: 2 April 2024

Revised: 10 May 2024

Accepted: 16 May 2024

Published: 19 May 2024



Copyright: © 2024 by the authors.

Licensee MDPI, Basel, Switzerland.

This article is an open access article

distributed under the terms and

conditions of the Creative Commons

Attribution (CC BY) license ([https://creativecommons.org/licenses/by/](https://creativecommons.org/licenses/by/4.0/)

[https://creativecommons.org/licenses/by/](https://creativecommons.org/licenses/by/4.0/)

4.0/).

1. Introduction

Reducing greenhouse gas emissions from the transport sector, increasing fuel efficiency, and bringing environmentally friendly vehicles to the market have become the main objectives of the car industry [1]. Consequently, the hybridisation of conventional vehicles presents a variety of potential avenues for enhancing the vehicle's fuel efficiency. These include storing braking energy in the battery for later use for propulsion [2,3], utilising engine power at higher efficiency zones, and otherwise using the electric motor for propulsion. Furthermore, the integration of an electric motor enables a reduction in the size of the engine, thereby enhancing efficiency through the operation in higher load ranges [4].

Optimising the size of powertrain components [5,6] and developing efficient control logic for power distribution [7] between the engine and the electric motor, while taking into account the vehicle architecture, powertrain dynamics, and power source characteristics, can significantly improve HEV fuel efficiency.

There is extensive literature on the HEV controller design [8–11]. In the literature, two main groups of control strategies are used to develop EMS for HEVs [7]. These are the rule-based (RBCS) and the optimisation-based control strategies (OBCS). The RBCS is a relatively basic control strategy that is simple to implement, as it employs a series

of static predetermined rules to manage the power split between the sources [12]. The rules are established by the experience of the engineers. The RBCS relies upon a series of static parameters to select driving modes, rendering it less adaptable to dynamic changes in the driving context [13]. Conversely, the OBCS provides an optimal power split and utilises a cost function that is minimised over a constrained range. This results in a fast response to varying vehicle operating states. The OBCS can be further categorised into two sub-types: the Global Optimisation Control Strategy (GOCS) and the Instantaneous Optimisation Control Strategy (IOCS). The GOCS provides an optimal global solution for a defined driving scenario, but this solution requires a high computing time and memory, and it is only applicable when the complete driving scenario is known in advance [14]. As a consequence, it cannot be used as a real-time control strategy; rather, its solution can serve as a benchmark to improve existing online controls [15]. On the contrary, the IOCS minimises the cost function at every time instant [16]. This makes IOCS an online, thus a real-time, regulator, and provides a local minimum solution. One of the widely used methods to solve the instantaneous optimisation problem is the Equivalent Consumption Minimisation Strategy (ECMS). Paganelli et al. [17] were the first to use an ECMS as an EMS of the HEV. ECMS aims at minimising the total amount of equivalent fuel use, including the fuel consumed by the engine and the virtual amount of fuel used by EM. It is necessary to constrain the cost function considering the operating limits of the power sources and the fulfilment of the driver's power requirements. To ensure battery operation in charge-sustaining mode, an s-shaped penalty function is often used [18].

To determine the optimum power distribution between the combustion engine and the electric motor(s), models based on a forward or backward approach are used [19,20]. Both models take into account the equations of longitudinal vehicle dynamics. The traction or braking torque required to accelerate or decelerate the vehicle is calculated from the speed profile of the drive cycle. These values are then used in the controller to identify the optimal torque distribution [10,11]. Commonly employed optimisation-based control strategies, such as dynamic programming and equivalent consumption minimisation, seek to minimise a cost function that includes the torque of the internal combustion engine (ICE) and the battery state of charge [19,21,22]. In these control strategies, the inertia effect of the flywheel and crankshaft is either neglected [8,9] or considered within the vehicle's apparent mass [21].

Certainly, the engine generates additional torque to overcome its own inertia, mainly composed of the inertia of the crankshaft and flywheel. Thus, the inclusion of the inertia effect of the crankshaft and flywheel in the controller serves to precisely estimate the engine's actual operating point in its characteristic map. This leads to further improved distribution of the torque demand. Several works can be found in the literature that are dedicated to the accurate estimation of the actual fuel consumption of the engine by optimising the torque or the power split. In [23,24], the precision of HEV fuel economy calculation was improved by integrating a transient behaviour of the engine. Moreover, by incorporating the engine transient behaviour in the controller, the reduction in its transient operation was achieved, resulting in more stable operation. This transient behaviour of the engine is influenced by a combination of factors, and it is difficult to isolate each effect and establish accurate analytical relationships [25].

Pam et al. [26] demonstrated the effect of the inertia of the rotating components of the vehicle, including the wheels, the inertia of the engine, and the EM on the estimation of the fuel consumption for P2 hybrid vehicles. Four different cases were compared. Dynamic programming was used as the control strategy, as it allows convergence to an optimal solution for each case. These cases include performing simulations with different vehicle masses, such as (i) static vehicle mass (i.e., neglecting rotating inertia), (ii) dynamic mass (taking into account the gear ratio change), (iii) average gear ratio, and (iv) average mass at different gear ratios. The results showed that the fuel consumption error can be in the range of 0.25–11.1% (the higher value corresponds to the static mass) when compared to the dynamic gear change case.

The works that consider the transient operation of the engine [23,25,27,28] mainly apply transient correction factors to quasi-static fuel consumption [23,27] determined by extensive experimental data [25].

Different from vehicles driven by only ICE, the constant addition of engine inertia may introduce some error in the estimation of the torque requirements for the HEV. This is because the effect of the engine and electric motor exists only in their respective operating modes. When one of the power sources is disengaged, its inertia should not affect the total mass of the vehicle. Consequently, the work defining the influence of engine inertia on the fuel consumption of HEV can be considered a valid and meaningful actual contribution to the field.

In this paper, mid-size two clutch P2 HEV with off-centre EM configuration was employed (see Figure 1). In the off-centre layout, the EM is connected to the input shaft of the gearbox through the belt drive.) In the P2 configuration, the resistive effect of the engine during braking phases can be bypassed, as the engine can be decoupled through the use of a clutch C_0 between the internal combustion engine (ICE) and the electric motor (EM). This allows the EM to accumulate more energy during regenerative phases.

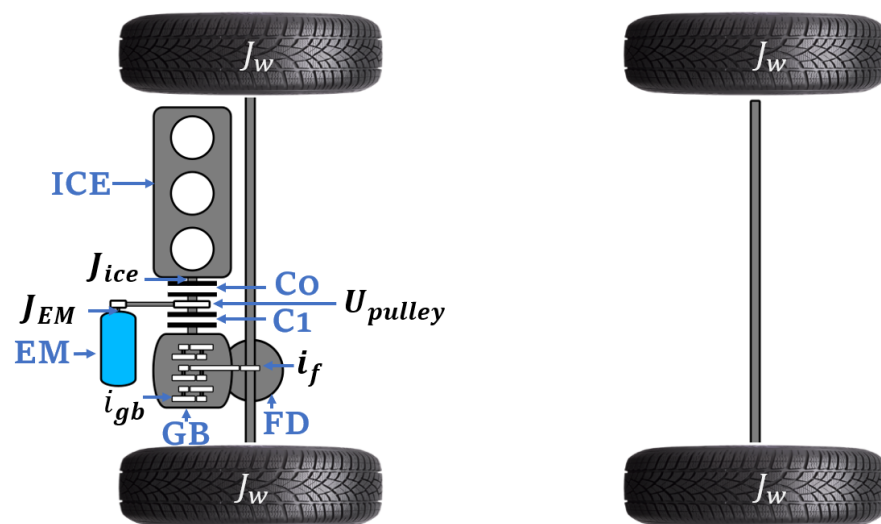


Figure 1. Layout of P2 HEV powertrain components. Components: ICE—internal combustion Engine, C0—main clutch, C1—secondary clutch, EM—electric motor, GB—gearbox, FD—final drive.

The developed vehicle simulator model considers the inertia of the entire powertrain components, i.e., from power sources to the wheels. This includes inertias of EM, ICE and four wheels. The torque split is implemented based on the required torque and speed at the input of the gearbox. Therefore, torque split optimisation can only be affected by the dynamics of the rotating components of power sources. The inertia of the crankshaft and flywheel is considerably higher than the rotary inertia of EM. Thus, the objective of this study is to demonstrate the influence of incorporating the engine inertia into the controller's cost function, while maintaining the vehicle performance model unchanged. It can be postulated that the incorporation of EM inertia into the cost function may result in a marginal enhancement of the torque split, although this may be accompanied by an increase in the complexity of the optimisation problem in the controller. Consequently, this paper is constrained to the consideration of engine inertia in the cost function of the controller.

The work adopts the ECMS as a control strategy due to its practical advantages, which take into account the inertial effect of the engine flywheel and crankshaft, as these components are critical in determining torque demand. The omission of consideration of these factors can result in inaccurate calculations and sub-optimal performance of the torque split controller. Consequently, this paper addresses two key objectives: firstly, to quantify the impact of crankshaft and flywheel inertia on fuel consumption in conventional

vehicles; and secondly, to develop an optimisation-based controller for hybrid electric vehicles (HEVs) that accounts for the inertia effect of rotational components of the engine.

The remainder of the paper is structured as follows. Section 2 is devoted to quantifying the impact of engine inertia on fuel consumption calculation in conventional ICE driving conditions. Section 3 outlines the influence of engine inertia in HEVs and presents an EMS designed to minimize this effect. The subsequent section involves a comparison of the obtained results with and without engine inertia. The conclusion summarizes the work and highlights the results obtained in this study.

2. Modelling the Vehicle Performance

A backward approach [19,20,22,29] was used to develop a vehicle simulator model for both a conventional vehicle and a P2 off-axis HEV (see Figure 2). The required torque output to move the vehicle on a given driving profile is calculated from the required vehicle speed, taking into account the vehicle architecture and the mechanical couplings in the powertrain. For the conventional vehicle simulation, only the thermal path depicted in Figure 2 is selected.

To follow the required speed profile $v = f(t)$, it is necessary to overcome vehicle inertia forces, the rolling resistance of the tyres, and the force of the aerodynamic drag. Therefore, the traction force F_{tr} on the wheel can be calculated as follows:

$$F_{tr} = M\dot{v} + Mg f_r + 1/2\rho_{air}C_d A_f v^2, \tag{1}$$

where M is the vehicle static mass, kg; \dot{v} is the vehicle longitudinal acceleration, m/s²; g is the the gravitational constant, m/s²; f_r is the tire rolling resistance coefficient, –; ρ_{air} is the air density, kg/m³; C_d is the aerodynamic drag coefficient, –; v is the vehicle longitudinal speed, m/s; and A_f is the frontal area of the vehicle, m².

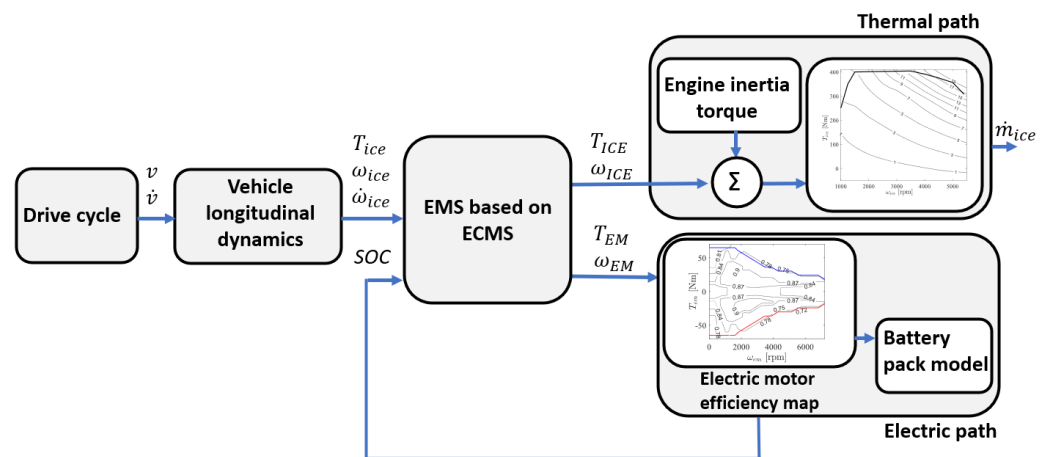


Figure 2. Layout of vehicle simulator model.

The tire model then converts the vehicle’s linear velocity v , acceleration \dot{v} , and required tractive force F_{tr} into axle rotational velocity (ω_w), angular acceleration ($\dot{\omega}_w$), and required torque (T_w), respectively. It should be noted that the rotational inertia of four wheels J_w is added to the torque required for the traction [19,22]:

$$T_w = F_{tr}R_e + 4J_w\dot{\omega}_w \tag{2}$$

where, R_e is the active radius of the tire that has been calculated from tire specifications [30] $\omega_w = v/R_e$ and $\dot{\omega}_w = \dot{v}/R_e$.

The transmission model consists of a mathematical representation of a six-speed gearbox, final gear, and differential. The inputs and outputs of the transmission model are interlinked as described in Equation (3). The required torque T_{req} is then split between ICE and EM [29]:

$$\begin{aligned}
 T_{req} &= \frac{T_w}{i_f \eta_f i_{gb} \eta_{gb}} \quad \text{if } (T_w > 0) \\
 T_{req} &= \frac{T_w \eta_f \eta_{gb}}{i_f i_{gb}} \quad \text{if } (T_w < 0) \\
 \omega_{req} &= \omega_w i_f i_{gb} \\
 \dot{\omega}_{req} &= \dot{\omega}_w i_f i_{gb}
 \end{aligned} \tag{3}$$

where i_f is the final gear ratio, η_f is the transmission efficiency of the final gear, i_{gb} is the gear ratio of the gearbox, and η_{gb} is the transmission efficiency of the gearbox.

3. Influence of Engine Inertia on Fuel Consumption of the Conventional Vehicle

The internal combustion engine model is based on open-source data from the Environmental Protection Agency for the 2016 Mazda CX9 2.5L Skyactive gasoline engine [31]. The main specifications of the vehicle are listed in Table 1. The conventional backward model has been validated using experimental results of the vehicle on the dynamometer by Argonne National Laboratory and is publicly available on [32]. The simulation model of the conventional vehicle comprises a number of subsystems, including the drive cycle, which defines the reference vehicle speed and acceleration; the vehicle dynamics, which are used to calculate the forces that resist vehicle motion; the transmission, which changes the values of torque and angular speed based on the speed ratio of the engaged gear; and the engine subsystem, which is modelled as a static map to compute the fuel consumption. The readers are respectfully requested to refer to previously published authors' paper [29] for a comprehensive description of the model and its experimental validation.

Table 1. Vehicle specifications of 2016 Mazda CX9. Data from [33].

Parameters	Value
Vehicle	Small SUV 4WD
Curb Weight	2041 kg
Frontal Area	2.4207 m ²
Transmission ratios	6-speed automatic
Gearbox (1st to 6th)	3.49; 1.99; 1.45; 1; 0.71; 0.6
Final drive	4.41
Engine	2.5L, GDI, I4
Power	169 kW @ 5000 rpm
Torque	310 Nm @ 2000 rpm
Engine inertia	0.373 kg m ²
Electric motor *	
Power	27 kW @ 4000 rpm
Torque	65 Nm @ 4000 rpm

* Notes: The original 2016 Mazda CX9 is a conventional vehicle. In this work, for simulation purposes, an electric motor is added to form a P2 off-axis HEV.

As stated earlier, the required engine output torque (T_{ice} is the torque generated at the input shaft of the gearbox to overcome resistance forces and the wheels' inertia) and angular velocity are calculated using the backward model based on the drive cycle request. In a further step, in addition to the required torque, the engine model calculates the torque

needed to overcome the inertia of the rotating parts by multiplying the inertia of the crankshaft and flywheel J_{ice} by the rotational acceleration of the crankshaft $\dot{\omega}_{ice}$. Thus, the engine's actual torque ($T_{ice,actual}$ including inertia torque of engine rotary components) is calculated as follows:

$$T_{ice,actual} = T_{ice} + \text{sign}(T_{ice})J_{ice}\dot{\omega}_{ice} \quad (4)$$

In this model, the P2 configuration is employed; thus, the resistive effect of the engine during braking phases can be avoided by the presence of a clutch between the flywheel and transmission. Consequently, in this configuration, the engine's output torque is either considered as zero or a positive value. When the engine does not contribute to propelling the vehicle ($\text{sign}(T_{ice})$ equals zero), it is decoupled from the transmission. In such cases, there is no need to account for engine inertia torque (the engine may be switched off or idling). However, if the engine remains connected to the transmission and provides torque for vehicle propulsion ($\text{sign}(T_{ice})$ equals 1), the engine inertia torque is appropriately included. Figure 3 demonstrates the variation of 2.5 L engine inertia torque throughout the UDDS driving cycle in the engine driving mode. The torque exhibits a notably high value (ranging from -28 to 30 Nm) during acceleration and braking phases while remaining insignificant during steady motion. Engine consumption is estimated instantly using actual engine torque and angular speed, using a steady-state engine map.

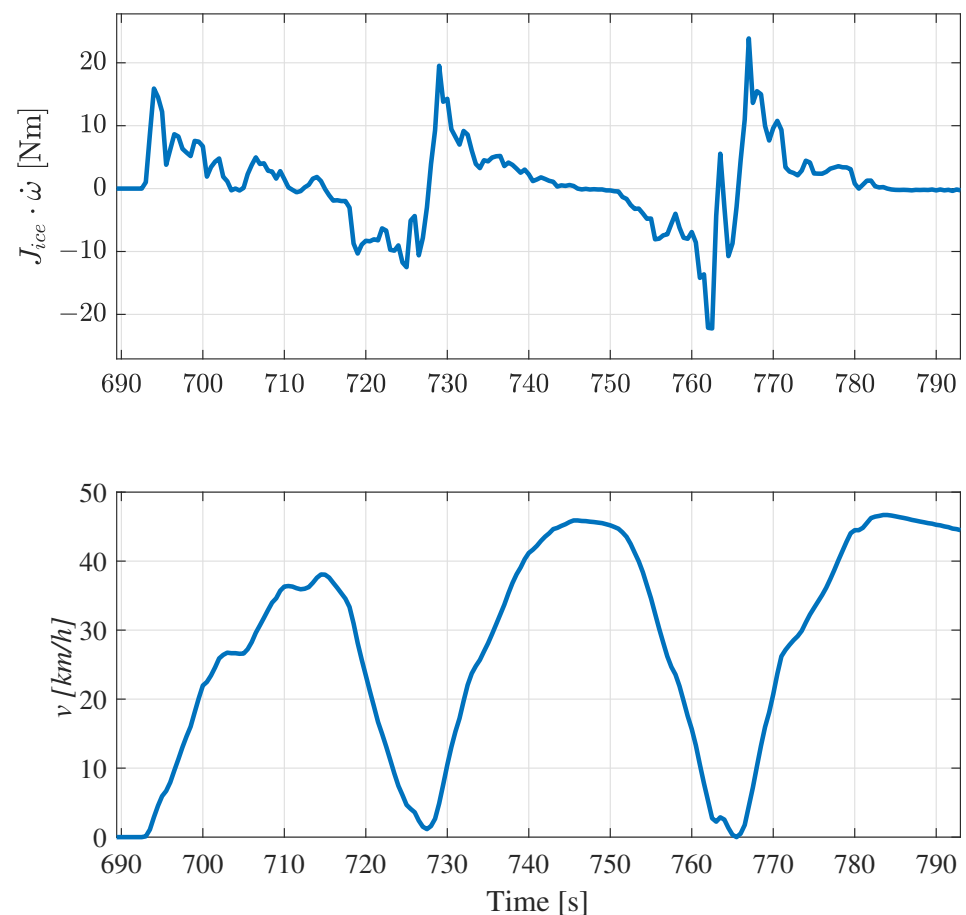


Figure 3. Engine inertia torque in UDDS cycle.

To investigate the effect of inertia on fuel consumption, we simulated the model with and without engine inertia and compared the total vehicle fuel consumption for UDDS, WLTC, and US06 driving cycles. According to the data, there is an increase in vehicle fuel consumption. Table 2 shows that the components of the engine inertia have a noticeable impact on fuel consumption. The fuel consumption required to overcome the

inertia of the engine's rotating components varies from 14 to 17 g in the considered driving cycles. This results in an additional 1.16–2% of fuel consumed due to engine inertia for one complete cycle. Cycle US06 was found to have the highest fuel usage to overcome engine inertia during the observed driving cycles, indicating that it is the most aggressive of the three cycles due to its numerous transient phases.

Table 2. A comparison of the fuel consumption results for the conventional vehicle with and without engine inertia.

Drive Cycle	FC without J_{ice}	FC with J_{ice}	Difference	Difference
	[g]	[g]	[g]	[%]
UDDS	685	699	14	2
US06	939	956	17	1.77
WLTC	1293	1308	15	1.16

4. Influence of Engine Inertia on Fuel Consumption of the HEV

To obtain an HEV model, a conventional vehicle model is combined with models of an electric motor, a battery, and an ECMS controller (Figure 2). The electric motor model includes its static efficiency map that can be obtained experimentally, using computer-aided engineering software tools or analytically from a single operating point data [34]. The EM model estimates the electrical power requirements from the battery for the requested EM operating condition. The battery model estimates the state of charge (SOC) level from the power request, taking into account the pack configuration and characteristics. For a comprehensive understanding of the electric motor and battery pack model, please refer to [29]. To keep the focus on the contribution of the paper, the previously described content form [29] is not introduced.

4.1. Conventional ECMS

ECMS is an online real-time optimisation-based control strategy [17,22]. The cost function is the total fuel consumption rate \dot{m}_{total} that includes the engine fuel consumption rate \dot{m}_{ice} and the equivalent fuel consumption rate of the electric motor \dot{m}_{eqv} . Thus, the minimization of the total consumption based on the current input and the current state of the variables is the objective calculated as:

$$\dot{m}_{total}(T_{ice}, T_{em}) = \dot{m}_{ice}(T_{ice}, \omega_{ice}) + \dot{m}_{eqv}(T_{em}, \omega_{em}) \quad (5)$$

The engine fuel consumption \dot{m}_{ice} is determined by the steady-state map and described by the polynomial fit equation (Equation (6)) as a function of the engine torque and angular velocity. The experimental data from [31] for the 2016 Mazda CX9 2.5L Skyactive gasoline engine are used for this purpose:

$$\begin{aligned} \dot{m}_{ice}(T_{ice}, \omega_{ice}) = & p_{00} + p_{10}\omega_{ice} + p_{01}T_{ice} + p_{20}\omega_{ice}^2 + p_{11}\omega_{ice}T_{ice} + p_{02}T_{ice}^2 + \\ & + p_{21}\omega_{ice}^2T_{ice} + p_{12}\omega_{ice}T_{ice}^2 + p_{03}T_{ice}^3 \end{aligned} \quad (6)$$

where p_{ij} is the coefficient of polynomial fit.

The term \dot{m}_{eqv} of the EM equivalent fuel consumption in Equation (5) is calculated by virtually comparing the power from the electric path to power obtained from the thermal one (Figure 4). In such a way, the amount of virtual fuel consumed to generate such electric power can be calculated [17].

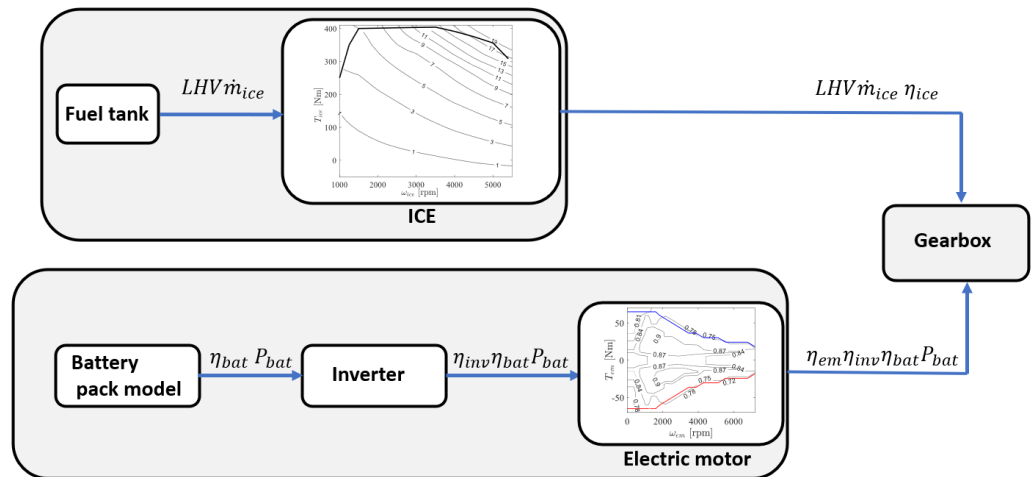


Figure 4. Power flow from the electric and thermal sources to the gearbox input.

The mechanical power generated by the thermal path when the engine consumes \dot{m}_{eqv} fuel considering its mean efficiency η_{ice} and lower heating value of gasoline LHV :

$$P_{ice} = \eta_{ice} LHV \dot{m}_{eqv} \quad (7)$$

The mechanical traction power generated by the electric path P_{em} considering the mean efficiency of path (electric motor η_{em} , inverter η_{inv} and battery η_{bat}):

$$P_{em} = \eta_{em} \eta_{inv} \eta_{bat} P_{bat} \quad (8)$$

By equating the mechanical powers in Equations (7) and (8), an equivalent conversion factor (s_{eqv}) can be evaluated to convert electrical power consumption into equivalent fuel consumption. Equation (9) shows the calculation of this factor for traction and braking modes, under the assumption that the efficiency of the paths is the same for both modes:

$$s_{eqv} = \begin{cases} \frac{1}{LHV \eta_{ice} \eta_{em} \eta_{inv} \eta_{bat}} & \text{if } (P_{bat} > 0) \\ \frac{\eta_{em} \eta_{inv} \eta_{bat}}{LHV \eta_{ice}} & \text{if } (P_{bat} < 0) \end{cases} \quad (9)$$

Then, the equivalent fuel usage of EM can be obtained as:

$$\dot{m}_{eqv}(P_{bat}) = P_{em} s_{eqv} = T_{em} \omega_{em} s_{eqv} \quad (10)$$

The constraints in terms of engine and EM operating envelopes need to be considered while satisfying the driver’s torque demand. Therefore, the following constraints are applied to the problem:

$$\begin{aligned} T_{req} &= T_{em} U_{pulley} + T_{ice} \\ 0 &\leq T_{ice} \leq T_{ice.max} \\ T_{gen.max} &\leq T_{em} \leq T_{em.max} \end{aligned} \quad (11)$$

where T_{req} is the requested torque at the gearbox input level that needs to be split between the power sources, U_{pulley} is the transmission ratio of the pulley of the P2 off-axis configuration, $T_{em.max}$ and $T_{gen.max}$ are the maximum torques of the electric machine in traction and braking modes, and $T_{ice.max}$ is the engine maximum torque.

In the Mild HEV system, where the charge-sustaining mode is commonly used, the SOC level must be maintained at the same level at the start and end of the driving cycle. To guarantee this operating condition of the battery, at higher SOC, the electric traction

should be used more. This can be implemented using an *s*-shaped penalty function on SOC integrated into the cost function as proposed in [18], as follows:

$$P_{SOC} = 1 - 0.15 \overline{SOC}^3 \quad (12)$$

where \overline{SOC} is normalized SOC:

$$\overline{SOC} = \frac{2SOC - (SOC_{high} + SOC_{low})}{SOC_{high} - SOC_{low}} \quad (13)$$

Then, the cost function can then be updated as:

$$\dot{m}_{total} = \dot{m}_{ice}(T_{ice}, \omega_{ice}) + P_{SOC} \dot{m}_{eqv}(T_{em}, \omega_{em}) \quad (14)$$

The optimum solution for the torque split between the motor and EM can be obtained by minimizing the cost function in Equation (14) over the constraints in Equation (11). However, as the engine's actual operation point is slightly different from the one set by the controller, the inertia torque is added to the requested torque while computing the fuel consumption in the engine model as shown in Figure 2.

4.2. ECMS Including Inertia Effect of the Engine

Increasing the accuracy of the estimation of the actual engine operating state in the cost function improves the determination of the optimal torque split in the HEV. Therefore, the engine inertia components are included in the ECMS cost function to achieve a better torque split between ICE and EM. The objective function is then updated with the additional inertia term for the engine torque:

$$\dot{m}_{total} = \dot{m}_{ice}(T_{ice} + \text{sign}(T_{ice})J_{ice}\dot{\omega}_{ice}, \omega_{ice}) + P_{SOC} \dot{m}_{eqv}(P_{bat}) \quad (15)$$

The constraints can also be updated as:

$$\begin{aligned} T_{req} &= T_{em} U_{pulley} + T_{ice} + \text{sign}(T_{ice})J_{ice}\dot{\omega}_{ice} \\ 0 &\leq T_{ice} + \text{sign}(T_{ice})J_{ice}\dot{\omega}_{ice} \leq T_{ice.max} \\ T_{gen.max} &\leq T_{em} \leq T_{em.max} \end{aligned} \quad (16)$$

With the cost function in Equation (15), the ECMS manages the torque distribution by taking into account the effect of engine inertia in advance. This should further improve the efficiency of the controller and save fuel.

5. Results and Discussion

The simulations are carried out with and without the inertia effect of the engine. The results obtained under the two ECMS controllers for engine torque, EM torque, engine fuel consumption and their speeds are compared as shown in Figure 5. A graphical illustration of a comparison of the results for UDDS cycle is given in Figure 6.

As can be observed from Figure 6, there is a notable improvement in the stability of engine operations, when the inertia effect is included in the ECMS cost function (blue line), particularly at the peaks of the torque profile. Given that the dynamic contributions of the engine components are significant in the high-acceleration zones, it is evident that they contribute additional peaks to the engine torque. In addition, the operation of the ICE at low-torque and low-speed operating conditions where the engine inertia torque is significantly high is reduced. Typically, the ICE operates at very low efficiency at such low-torque and low-speed operating conditions. Therefore, EM operation is preferable for these ranges, as it operates at a higher efficiency. Consequently, the energy usage to overcome the inertia effect of the crankshaft and flywheel can be avoided in these ranges. The torque profile of the EM indicates that it takes on an additional portion of the required torque. This

demonstrates that the engine’s stable operation is primarily achieved by reducing the inertia effects. In particular, the moments of inertia are significantly reduced at 692–698 s, 727–730 s and 760–769 s by using EM for traction. This means that the utilisation of EM power in the HEV is further optimised by incorporating the inertia effect of the engine in the controller. This leads to an improvement in the overall efficiency of the HEV system. The simulation results in terms of HEV fuel consumption demonstrate that including engine dynamics in the cost function leads to a fuel economy improvement of the vehicle. The results are summarised in Table 3. The maximum fuel saving (1.3%) can be achieved in the UDDS cycle, as it has more acceleration phases than the other tested driving scenarios. These findings are consistent with those reported by Pam et al. [26] in their study of the average mass model.

The incorporation of the dynamic behaviour of rotating engine components into the cost function has been demonstrated to result in a significant enhancement of the power distribution for hybrid electric vehicle (HEV) systems. The modification to the energy management of the system described above is relatively simple and does not require additional modelling of the engine characteristics, as does a transient engine model. Indeed, developing a transient model of an engine requires regression analysis on acquired data obtained in special laboratory conditions, which may not be available for every case. Consequently, the incorporation of inertial effects into the cost function is relatively easy to implement, enabling the inclusion of a part of the transient behaviour of the engine.

Table 3. Comparison of HEV vehicle fuel consumption with and without considering engine inertia effects in the ECMS controller on different driving cycles.

Drive Cycle	ECMS without J_{ice}	ECMS with J_{ice}	Fuel Saving		CO ₂ Reduction
	[g]	[g]	[g]	[%]	[g/km]
UDDS	611	602	9	−1.3	2.34
US06	852	842.9	9.1	−0.9	2.22
WLTC	1185	1181	4	−0.3	1.13

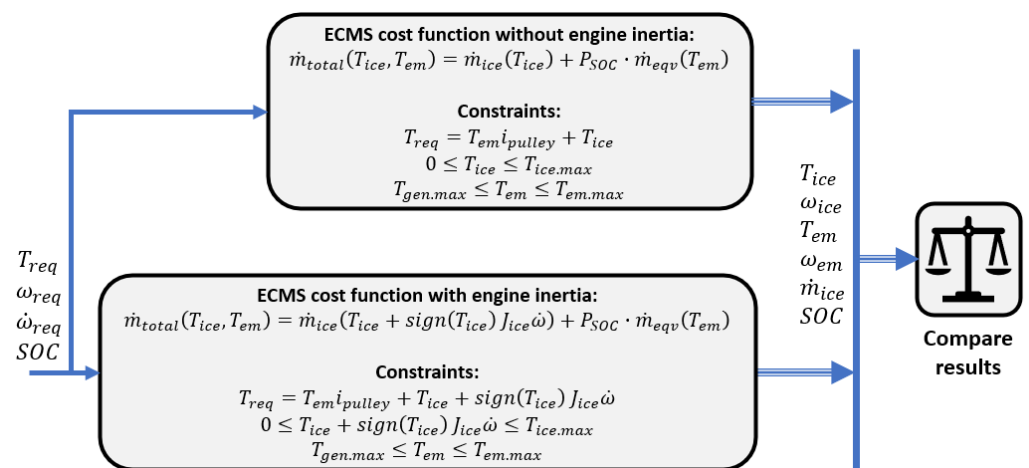


Figure 5. Comparison of two ECMS control outputs.

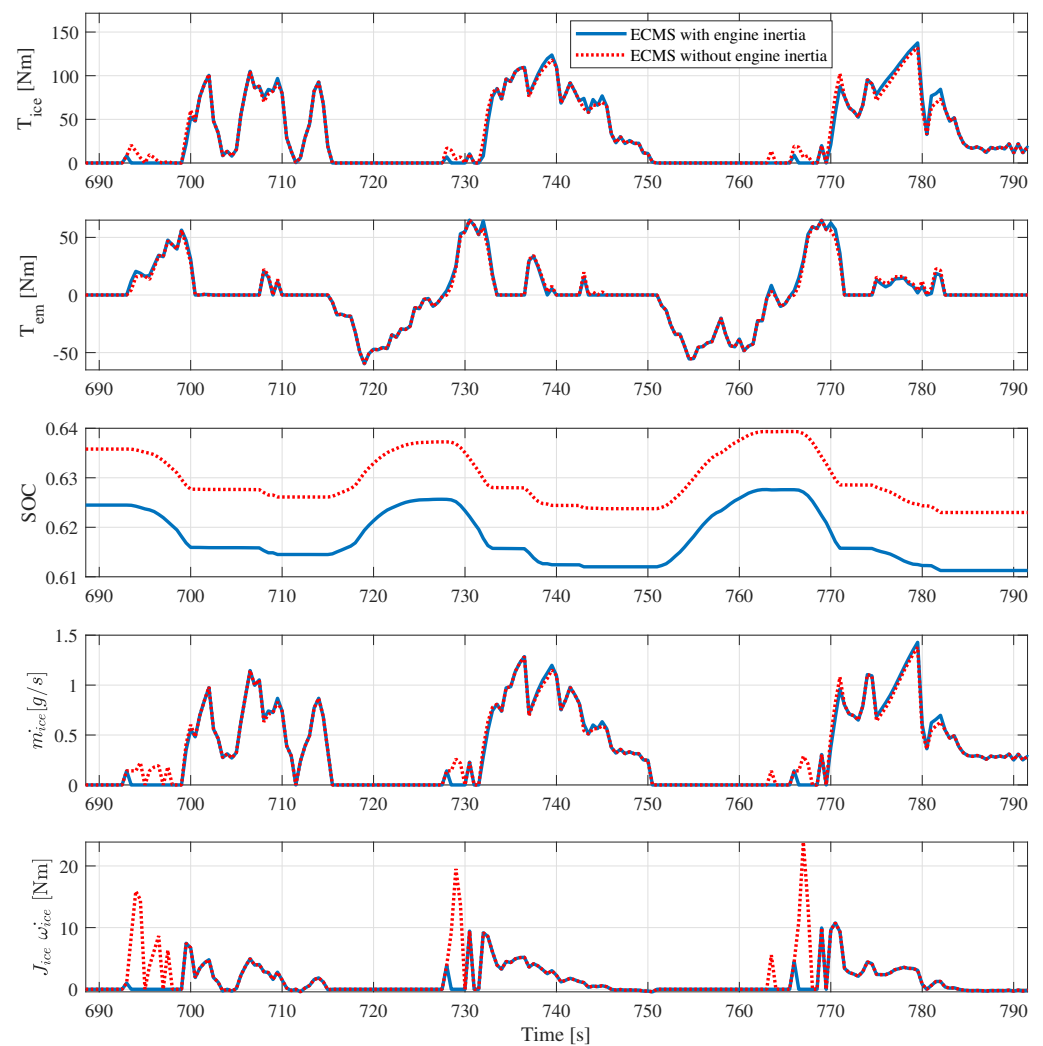


Figure 6. Comparison of HEV vehicle fuel consumption with and without considering inertia effects in the ECMS controller. In the order of appearance: ICE torque, EM torque, battery SOC, ICE fuel consumption, and engine inertia torque.

6. Conclusions

The initial phase of this research work involved an analysis of the impact of engine inertia on the fuel consumption of conventional vehicles. The simulation results indicated that engine inertia plays a significant role in the fuel consumption of conventional vehicles during high-acceleration phases. It was observed that the fuel consumption of the Mazda CX9 2016 can vary from 1.16% to 2% over the WLTC, UDDS and US06 driving cycles to overcome the effect of engine inertia. The largest discrepancy was observed in the UDDS driving cycle, which encompasses a greater proportion of transient and rapidly accelerated driving phases than the other cycles.

In an attempt to monitor this effect in P2 Mild HEVs, the traditional ECMS algorithm was developed as an energy management system for the vehicle. Subsequently, a novel controller was modified by incorporating the inertial effect of the engine crankshaft and flywheel into the ECMS controller algorithm. A simulation was conducted to assess the performance of the HEV under the control of the developed supervisor controllers, namely, the traditional ECMS and ECMS including inertial effects, for the same driving cycles.

The results demonstrated that incorporating the dynamics of the engine's rotating components into the cost function enhanced the precision of the fuel consumption estimation by the controller, thereby improving the distribution of optimal power in the HEV. Furthermore, the inclusion of the inertial effect in the controller stabilises the engine opera-

tion. In particular, engine operation during startup phases with high accelerations where low torque and low speeds are required is of particular concern, as the engine operates at very low efficiency during this period. The EM power was alternatively employed during these phases. This optimises the utilisation of EM power for the HEV in charge-maintaining mode. Consequently, the HEV demonstrated fuel savings of 9, 9.1, and 4 g in the UDDS, US06, and WLTC cycles, respectively. This equates to a reduction in CO₂ emissions of 2.34, 2.22 and 1.13 g/km, respectively. The greatest improvement can be observed in more challenging driving cycles as UDDS and US06 cycles.

This paper proposed optimisation of the power distribution of HEV by considering the inertia effect of engine components in the ECMS controller. Indeed, ECMS is an online controller that provides a local optimal solution. In contrast, dynamic programming provides a global optimal solution since it minimises the cost function over the entire cycle. It is anticipated that the effect of inertial components will be even more noticeable, including the dynamics of power sources in EMS, when dynamic programming is applied. Furthermore, the transient correction factor is expected to enhance the precision of the calculation of engine fuel consumption, thereby reducing fuel consumption due to engine inertia.

Author Contributions: Conceptualization, S.R., G.Y., A.T. and A.M.; methodology, S.R. and G.Y.; software, G.Y.; validation, S.R., G.Y. and A.T.; formal analysis, S.R. and A.T.; investigation, G.Y. and S.R.; resources S.R. and A.M.; data curation, G.Y. and S.R.; writing—original draft preparation, G.Y.; writing—review and editing, S.R., G.Y., A.T. and A.M.; visualization, S.R. and G.Y.; supervision, S.R., A.T. and A.M.; project administration, A.M., A.T. and S.R.; funding acquisition, S.R. All authors have read and agreed to the published version of the manuscript.

Funding: This research received no external funding.

Data Availability Statement: These data were derived from the following resources available in the public domain: <https://www.epa.gov/vehicle-and-fuel-emissions-testing/combining-data-complete-engine-alpha-maps> and <https://www.anl.gov/taps/d3-2016-mazda-cx9>, accessed on 1 April 2024.

Conflicts of Interest: The authors declare no conflicts of interest.

Abbreviations

The following abbreviations are used in this manuscript:

GDI	Gasoline Direct Injection
HEV	Hybrid Electric Vehicle
TLA	Three-letter acronym
LD	Linear dichroism

References

1. Buberger, J.; Kersten, A.; Kuder, M.; Eckerle, R.; Weyh, T.; Thiringer, T. Total CO₂-Equivalent Life-Cycle Emissions from Commercially Available Passenger Cars. *Renew. Sustain. Energy Rev.* **2022**, *159*, 112158. [CrossRef]
2. Quarto, M.L.; Goodnight, N. *Light Duty Hybrid and Electric Vehicles (Master Automotive Technician)*; CDX Learning Systems; Jones and Bartlett: Burlington, MA, USA, 2023; ISBN 9781284198010.
3. van Keulen, T.; de Jager, B.; Kessels, J.; Steinbuch, M. Energy Management in Hybrid Electric Vehicles: Benefit of Prediction. *IFAC Proc.* **2010**, *43*, 264–269. [CrossRef]
4. Ebbesen, S.; Elbert, P.; Guzzella, L. Engine Downsizing and Electric Hybridization Under Consideration of Cost and Drivability. *Oil Gas Sci. Technol. D'Ifp Energies Nouv.* **2012**, *68*, 109–116. [CrossRef]
5. Sanjarbek, R.; Mavlonov, J.; Mukhitdinov, A. Analysis of the Powertrain Component Size of Electrified Vehicles Commercially Available on the Market. *Commun. Sci. Lett. Univ. Zilina* **2022**, *24*, B74–B86. [CrossRef]
6. Castellazzi, L.; Ruzimov, S.; Bonfitto, A.; Tonoli, A.; Amati, N. A Method for Battery Sizing in Parallel P4 Mild Hybrid Electric Vehicles. *SAE Int. J. Electrified Veh.* **2021**, *11*, 97–111. [CrossRef]
7. Xue, Q.; Zhang, X.; Teng, T.; Zhang, J.; Feng, Z.; Lv, Q. A Comprehensive Review on Classification, Energy Management Strategy, and Control Algorithm for Hybrid Electric Vehicles. *Energies* **2020**, *13*, 5355. [CrossRef]
8. Wang, S.; Qin, D. Online Control Strategy for Plug-In Hybrid Electric Vehicles based on an improved global optimization Algorithm. *Appl. Sci.* **2020**, *10*, 8352. [CrossRef]

9. Serrao, L.; Onori, S.; Rizzoni, G. ECMS as a realization of Pontryagin's minimum principle for HEV control. In Proceedings of the 2009 American Control Conference Hyatt Regency Riverfront, St. Louis, MO, USA, 10–12 June 2009. [CrossRef]
10. Musardo, C.; Rizzoni, G.; Guezennec, Y.; Staccia, B. A-ECMS: An adaptive algorithm for hybrid electric vehicle energy management. *Eur. J. Control* **2005**, *11*, 509–524. [CrossRef]
11. Li, H.; Hu, X.; Fu, B.; Wang, J.; Zhang, F.; Zhou, Y. Effective optimal control strategy for hybrid electric vehicle with continuously variable transmission. *Adv. Mech. Eng.* **2019**, *11*, 1687814018824811. [CrossRef]
12. Peng, J.K.; Fan, H.; He, H.W.; Pan, D. A Rule-based energy management strategy for a plug-in hybrid school bus based on a controller area network bus. *Energies* **2015**, *8*, 5122–5142. [CrossRef]
13. Zhang, F.; Wang, L.; Coskun, S.; Pang, H.; Cui, Y.; Xi, J. Energy Management Strategies for Hybrid Electric Vehicles: Review, Classification, Comparison, and Outlook. *Energies* **2020**, *13*, 3352. [CrossRef]
14. Wang, R.; Lukic, S.M. Dynamic programming technique in hybrid electric vehicle optimization. In Proceedings of the 2012 IEEE International Electric Vehicle Conference, Greenville, SC, USA, 4–8 March 2012. [CrossRef]
15. Tribioli, L.; Barbieri, M.; Capata, R.; Enrico, S.; Elio, J.; Gino, B. A Real Time Energy Management Strategy for Plug-in Hybrid Electric Vehicles based on Optimal Control Theory. *Energy Procedia* **2014**, *45*, 949–958. [CrossRef]
16. Waldman, C.; Gurusubramanian, S.; Fiorentini, L.; Canova, M. A model-based supervisory energy management strategy for a 12 V vehicle electrical system. *Control. Eng. Pract.* **2015**, *44*, 20–30. [CrossRef]
17. Paganelli, G.; Delprat, S.; Guerra, T.M.; Rimaux, J.; Santin, J.J. Equivalent Consumption Minimization Strategy for Parallel Hybrid Powertrains. In Proceedings of the Vehicular Technology Conference. IEEE 55th Vehicular Technology Conference. VTC Spring 2002 (Cat. No. 02CH37367), Birmingham, AL, USA, 6–9 May 2002.
18. Liu, X.; Qin, D.; Wang, S. Minimum Energy Management Strategy of Equivalent Fuel Consumption of Hybrid Electric Vehicle Based on Improved Global Optimization Equivalent Factor. *Energies* **2019**, *12*, 2076. [CrossRef]
19. Guzzella, L.; Sciarretta, A. *Vehicle Propulsion Systems*; Springer: Berlin/Heidelberg, Germany, 2013. [CrossRef]
20. Horrein, L.; Bouscayrol, A.; Delarue, P.; Verhille, J.N.; Mayet, C. Forward and Backward Simulations of a Power Propulsion System. *IFAC Proc.* **2012**, *45*, 441–446. [CrossRef]
21. Ehsani, M.; Gao, Y.; Emadi, A. *Modern Electric, Hybrid Electric, and Fuel Cell Vehicles*; CRC Press: Boca Raton, FL, USA, 2017. [CrossRef]
22. Onori, S.; Serrao, L.; Rizzoni, G. *Hybrid Electric Vehicles*; Springer: London, UK, 2016. [CrossRef]
23. Yakhshilikova, G.; Ruzimov, S.; Ezemobi, E.; Tonoli, A.; Amati, N. Development of Optimization Based Control Strategy for P2 Hybrid Electric Vehicle including Transient Characteristics of Engine. *Appl. Sci.* **2022**, *12*, 2852. [CrossRef]
24. He, H.; Shou, Y.; Song, J. An improved A-ECMS energy management for plug-in hybrid electric vehicles considering transient characteristics of engine. *Energy Rep.* **2023**, *10*, 2006–2016. [CrossRef]
25. Dekraker, P.; Stuhldreher, M.; Kim, Y. Characterizing factors influencing SI engine transient fuel consumption for vehicle simulation in ALPHA. *SAE Int. J. Engines* **2017**, *10*, 529–540. [CrossRef]
26. Pam, A.; Bouscayrol, A.; Fiani, P.; Faval, F. Comparison of different models for energy management strategy design of a parallel hybrid electric vehicle: Impact of the rotating masses. *IET Electr. Syst. Transp.* **2021**, *11*, 36–46. [CrossRef]
27. Hao, G.; Hui, J. Fuel Consumption Model Optimization Based on Transient Correction. *Energy* **2019**, *169*, 508–514.
28. Lindgren, M. A Transient Fuel Consumption Model for Non-road Mobile Machinery. *Biosyst. Eng.* **2005**, *91*, 139–147. [CrossRef]
29. Yakhshilikova, G.; Ezemobi, E.; Ruzimov, S.; Tonoli, A. Battery Sizing for Mild P2 HEVs Considering the Battery Pack Thermal Limitations. *Appl. Sci.* **2021**, *12*, 226. [CrossRef]
30. Genta, G. *Motor Vehicle Dynamics: Modeling and Simulation*; Series on Advances in Mathematics for Applied Sciences; World Scientific: Singapore, 1997. [CrossRef]
31. Available online: <https://www.epa.gov/vehicle-and-fuel-emissions-testing/combining-data-complete-engine-alpha-maps> (accessed on 31 January 2024).
32. Available online: <https://www.anl.gov/es/energy-systems-d3-2016-mazda-cx9> (accessed on 31 January 2024).
33. Available online: https://www.thecarconnection.com/specifications/mazda_cx-9_2016 (accessed on 31 January 2024).
34. Ciampolini, M.; Fazzini, L.; Berzi, L.; Ferrara, G.; Pugi, L. Simplified Approach for Developing Efficiency Maps of High-Speed PMSM Machines for Use in EAT Systems Starting from Single-Point Data. In Proceedings of the 2020 IEEE International Conference on Environment and Electrical Engineering and 2020 IEEE Industrial and Commercial Power Systems Europe, IEEEIC/I and CPS Europe 2020, Madrid, Spain, 9–12 June 2020; p. 9160775. [CrossRef]

Disclaimer/Publisher's Note: The statements, opinions and data contained in all publications are solely those of the individual author(s) and contributor(s) and not of MDPI and/or the editor(s). MDPI and/or the editor(s) disclaim responsibility for any injury to people or property resulting from any ideas, methods, instructions or products referred to in the content.